

# A $\pi$ -Conjugated System with Flexibility and Rigidity That Shows Environment-Dependent RGB Luminescence

Chunxue Yuan,<sup>†</sup> Shohei Saito,<sup>\*,†,‡</sup> Cristopher Camacho,<sup>†</sup> Stephan Irle,<sup>\*,†,⊥</sup> Ichiro Hisaki,<sup>§</sup> and Shigehiro Yamaguchi<sup>\*,†,⊥</sup>

<sup>†</sup>Department of Chemistry, Graduate School of Science, and <sup>⊥</sup>Institute of Transformative Bio-Molecules (WPI-ITbM), Nagoya University, Furo, Chikusa, Nagoya 464-8602, Japan

<sup>‡</sup>PRESTO, Japan Science and Technology Agency (JST), Furo, Chikusa, Nagoya 464-8602, Japan

<sup>§</sup>Department of Material and Life Science, Graduate School of Engineering, Osaka University, Yamadaoka, Suita, Osaka 565-0871, Japan

## S Supporting Information

**ABSTRACT:** We have designed and synthesized a  $\pi$ -conjugated system that consists of a flexible and nonplanar  $\pi$  joint and two emissive rigid and planar wings. This molecular system exhibits respectively red, green, and blue (RGB) emission from a single-component luminophore in different environments, namely in polymer matrix, in solution, and in crystals. The flexible unit gives rise to a dynamic conformational change in the excited state from a nonplanar V-shaped structure to a planar structure, leading to a dual fluorescence of blue and green colors. The rigid and planar moieties favor the formation of a two-fold  $\pi$ -stacked array of the V-shaped molecules in the crystalline state, which produces a red excimer-like emission. These RGB emissions are attained without changing the excitation energy.

Research on  $\pi$ -conjugated systems has taken a leading role in the development of organic electronics.<sup>1</sup> Among a wide variety of molecular structures developed to date, the flexible  $\pi$  frameworks have been the focus of intensive studies. As exemplified by chemistry of cyclooctatetraene,<sup>2</sup> corannulene,<sup>3</sup> sumanene,<sup>4</sup> twisted perylene bisimide,<sup>5</sup> and expanded porphyrins,<sup>6</sup> their dynamic molecular motions can be the basis of various kinds of molecule-based functions.<sup>7</sup> However,  $\pi$  systems composed only of a flexible moiety often lose intrinsic advantages of the aromatic systems, such as luminescent properties and  $\pi$ -stacking ability. Their dynamic motion sometimes accelerates the nonradiative decay process from the excited state, which results in the quenching of emission.<sup>8</sup> In addition, the flexible  $\pi$  skeletons are apt to prevent the formation of a tightly  $\pi$ -stacked structure due to their low planarity.<sup>3b,9</sup>

We have now designed a new  $\pi$ -conjugated molecule **1** that consists of a flexible  $\pi$  moiety and two emissive rigid wings (Figure 1). The combination of the flexibility and rigidity imparts two remarkable characteristics to the skeleton. One is a dual monomer fluorescence based on a dynamic conformational change in the excited state, which is different from the mechanism of the well-investigated TICT or PICT (twisted/planarized intramolecular charge transfer) systems with a

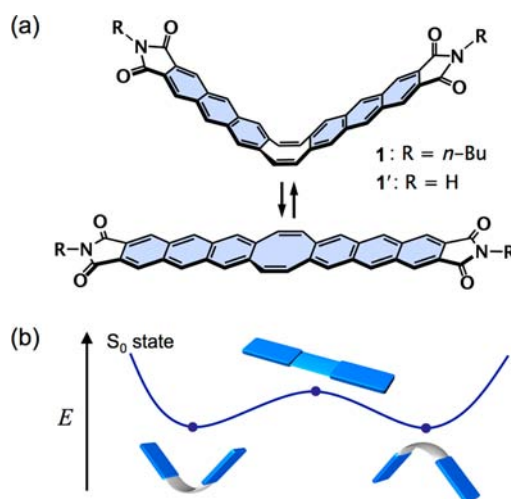


**Figure 1.** Conformational change of **1** with flexible and rigid  $\pi$  scaffolds, which perturbs the  $\pi$ -conjugation.

rotatable single bond.<sup>10</sup> The other one is a strong “two-fold”  $\pi$ -stacking ability of the V-shaped conformers. As a result, red, green, and blue emission was realized from the single organic luminophore in different environments. Since the three primary colors have significantly different energies, RGB luminescence without changing the excitation energy is quite limited.<sup>11,12</sup>

The design of our molecular system **1** is illustrated in Figure 1a. As the rigid wings, an anthraceneimide framework was selected due to its intense fluorescence, high planarity, and high chemical stability. The two wings are bridged by two *cis*-olefins to form an eight-membered ring. This central ring can be formally regarded as a cyclooctatetraene (COT) framework, which is a classical flexible  $\pi$ -conjugated skeleton.<sup>2,7d-f</sup> In conjunction with the tub-to-tub inversion of the COT moiety, the hybrid  $\pi$  system **1** is expected to undergo a “flapping” of the wings. The planar conformer as the transition state is 0.33 eV (= 7.7 kcal/mol) higher in energy than the V-shaped conformer, according to the DFT (B3LYP/6-31G(d)) calculation<sup>13</sup> on the  $S_0$  ground state of a model compound **1'**

Received: April 27, 2013

Published: May 30, 2013

(Figure 1b). The electronic structure is significantly perturbed by this structural change. Whereas the  $\pi$ -conjugation between the two aromatic wings is almost disconnected in the nonplanar V-shaped geometry, the planar conformation has an effective  $\pi$ -conjugation over the entire molecule (Supporting Information (SI)). The synthesis of **1** was achieved using the acene elongation reactions<sup>14</sup> from 2,3,6,7-tetrakis(methoxycarbonyl)-9,10-dihydro-9,10-ethenoanthracene as the starting material in seven steps in 14% overall yield (SI).

The RGB triple-color luminescence of **1** is shown in Figure 2. First, a green emission was observed from **1** in various common

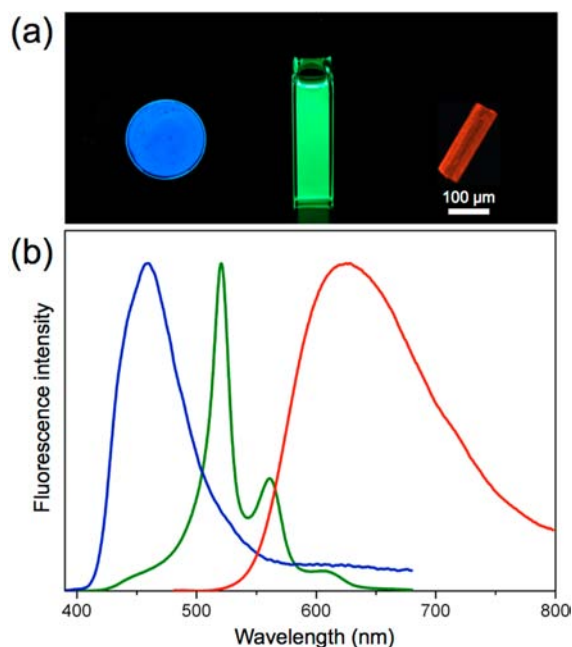


**Figure 2.** (a) RGB emissions of **1** in PMMA matrix (blue), in CH<sub>2</sub>Cl<sub>2</sub> solution (green), and in the crystalline state (red). Photographs under a 365 nm ultraviolet lamp irradiation. (b) The corresponding three luminescence spectra of **1** in the visible region.  $\lambda_{\text{ex}} = 350, 350,$  and  $450$  nm for blue, green, and red emission spectra, respectively. The same red emission band was observed even when  $\lambda_{\text{ex}} = 350$  nm.

organic solvents (SI). In CH<sub>2</sub>Cl<sub>2</sub>, the fluorescence maximum wavelength  $\lambda_{\text{em}}$  was 520 nm ( $\lambda_{\text{ex}} = 350$  nm), accompanied by vibronic peaks at 561 and 611 nm as well as a weak shoulder band in a higher-energy region around 460 nm. The quantum yield and the emission lifetime were determined to be  $\Phi = 0.31$  and  $\tau = 11.8$  ns. The UV/visible absorption and excitation ( $\lambda_{\text{em}} = 520$  nm) spectra were almost identical to each other, showing an intense band around 330 nm together with lower-energy bands around 395 and 420 nm (SI). The large Stokes shift of  $4640\text{ cm}^{-1}$  suggested a significant conformational change in the excited state. Second, a blue fluorescence ( $\Phi = 0.09$ ) was observed in a poly(methyl methacrylate) (PMMA) film containing **1** in a 1.0 wt% concentration. The fluorescence spectrum showed a single emission band at  $\lambda_{\text{em}} = 459$  nm. The lifetime of this emission band was determined to be  $\tau = 8.4$  ns. The absorption spectrum of the film showed lower-energy bands at 416 and 442 nm. The small Stokes shift of  $885\text{ cm}^{-1}$  indicated that the structural change observed in solution was considerably suppressed in the PMMA matrix. Third, a red luminescence was observed from the crystals of **1**, in which a broad and structureless band was delineated with the  $\lambda_{\text{em}}$  of 625 nm. The significant bathochromic shift, the lowest quantum

yield ( $\Phi = 0.06$ ) among the triple-color emissions, and the relatively long lifetime ( $\tau = 12\text{--}14$  ns) suggest an excimer-like emission of **1** in the crystals. All these RGB emission spectra were independent of the excitation wavelengths (SI). Therefore, these RGB luminescences can be produced by the UV light irradiation at the same wavelength only by changing the states of the luminophore, namely, in a solution, in a polymer matrix, or in crystals.

Compound **1** also showed a dramatic luminescent chromism between a green emission and a blue emission with increasing the viscosity of a 2-methyltetrahydrofuran (MTHF) solution at lower temperature (Figure 3a). The concentration of the

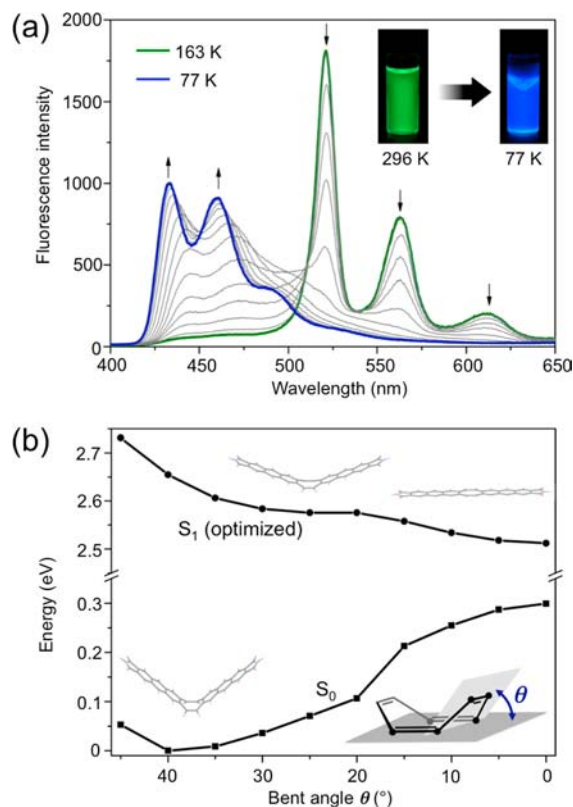


**Figure 3.** (a) Temperature-dependent fluorescence spectra of **1** in MTHF from 163 K (solution) to 77 K (glass).  $\lambda_{\text{ex}} = 350$  nm. (b) Calculated potential energy diagram for the S<sub>0</sub> and S<sub>1</sub> states of **1'** (see Figure 1) with fixed bent angle  $\theta$ . The constrained geometry optimization was performed in the S<sub>1</sub> state at the PBE0/def-SV(P) level.

solution at  $1.0 \times 10^{-6}$  M was low enough to preclude any intermolecular interaction. As the temperature decreased from 296 to 163 K, the fluorescence bands of the green emission gradually increased in intensity without any significant shifts in energy (SI). This behavior indicated that a nonradiative decay process from the S<sub>1</sub> excited state was retarded at the lower temperature, and thus the radiative decay process became more dominant to increase the fluorescence intensity. A further temperature reduction led to a decrease in intensity of the bands in the region from 500 to 650 nm, and the shoulder band in the shorter-wavelength region from 420 to 500 nm concomitantly increased (Figure 3a). At 133 K, both the green and blue emission bands were observed with comparable intensities to each other. Time-resolved fluorescence spectroscopy at this temperature showed that the blue emission band is

short-lived and thereafter the green emission band grows in (SI). The observation supports that the dynamic conformational change in the excited state is responsible for the blue and green “dual fluorescence”. At 77 K, compound **1** eventually exhibited a blue emission in the glass of MTHF. The fluorescence bands showed the  $\lambda_{\text{em}}$  of 433 nm with vibronic peaks at 460 and 491 nm. In comparison to the blue emission of **1** in the PMMA film, the spectrum in the MTHF glass state was structured and more blue-shifted, indicating that the conformational change of **1** in the excited state was suppressed to a greater extent in the glass state. On the other hand, the excitation spectra showed no temperature dependence from 296 to 77 K, regardless of the emission wavelengths (SI). As a result, the conformational flexibility should play an important role in the excited state on the fluorescence rather than in the ground state on the absorption properties.

To gain insights into the structural change in the excited state, theoretical calculations were conducted for the skeleton **1'** (Figure 1) using the TURBOMOLE quantum chemistry program<sup>15</sup> at the PBE0/def-SV(P) level of theory (Figure 3b). The geometries of **1'** in the  $S_1$  excited state were first optimized with the constraint of the COT bent angle  $\theta$  from 0 to 45° in 5-degree changes, and then the energy minimum points were fully optimized. The calculations demonstrated that, while the V-shaped structure with  $\theta = 40.6^\circ$  gave the lowest energy potential in the  $S_0$  ground state, the most stable geometry in the  $S_1$  excited state is a planar conformation ( $\theta = 0^\circ$ ) (SI). Thus, the “flapping” of the anthracene wings is the mode of conformational change upon photoexcitation.

Importantly, the  $S_1$  state has a local minimum at  $\theta = 22.8^\circ$  in addition to the global minimum at  $\theta = 0^\circ$  (SI). Radiative decay processes from these two states should be responsible for the dual fluorescence. Namely, the blue emission results from the shallow V-shaped excited state, while the green emission occurs from the planar excited state. The temperature dependence should be due to the restricted conformational change in the excited state at the lower temperature. In the range from 296 to 163 K, compound **1** undergoes the conformation change into the planar global minimum, which emits the green fluorescence. Upon approaching the freezing point of MTHF (137 K), the planarization in the excited state is gradually suppressed due to the increasing solvent viscosity at the lower temperature. Instead, the radiative decay process from the V-shaped local minimum becomes dominant, resulting in the blue fluorescence. Whereas the energy difference between the planar and shallow V-shaped conformations in the  $S_1$  state ( $\Delta E_{S_1,V-P}$ ) is as low as 0.062 eV, the planar conformer is much more unstable than the shallow V-shaped conformer by 0.21 eV in the  $S_0$  state. As a consequence, this structural change results in the significant change in the fluorescence colors (Figure 3). The small energy difference  $\Delta E_{S_1,V-P}$  can also explain the fact that the blue emission band was observed as a shoulder together with the green emission bands even at room temperature in solution. The  $\Delta E_{S_1,V-P}$  value implies that both the V-shaped and planar conformers can coexist in the ratio of 1:12 at 296 K in the excited state.

In contrast to the roles of the flexible COT core for gaining the dual fluorescence of the blue and green colors, the rigid and planar anthraceneimide wings in **1** are essential for gaining the red emission in the crystalline state. To elucidate the structural impact on the solid-state fluorescence, we next determined its crystal structure and compared its solid-state properties to that of an anthraceneimide monomer **2** as a reference compound.

Single crystals of **1** were obtained by careful recrystallization from a hot *o*-dichlorobenzene solution by slowly decreasing the temperature. A synchrotron radiation single crystal X-ray diffraction analysis demonstrated that **1** forms a stacked array structure in spite of the nonplanar V-shaped conformation with  $\theta = 44^\circ$  (Figure 4). In this structure, the planar wings are

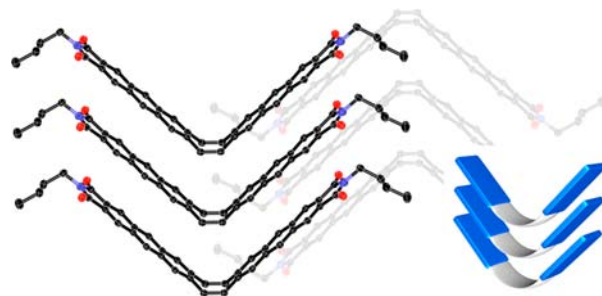


**Figure 4.** Two-fold  $\pi$ -stacked array structure of **1** in the crystalline state (50% probability for thermal ellipsoids).

stacked on both sides of the COT core. In other words, the central tub-shaped COT core forces the two-fold  $\pi$ -stacked array structure. The  $\pi$ -stacking of the anthraceneimide moieties is in a slipped fashion along the long axes of the anthracene moiety with the short interfacial distance of 3.39 Å. The strong  $\pi$ -stacking ability is responsible for the low solubilities in common organic solvents (for example, 7 mg/L in  $\text{CH}_2\text{Cl}_2$ , 60 mg/L in  $\text{CHCl}_3$ ) and readily formation of fibrous microcrystals (SI).

The reference compound **2**, a rigid substructure of **1**, showed blue emissions both in solution and in the PMMA matrix (Figure 5). The similarity in their emission spectra to each

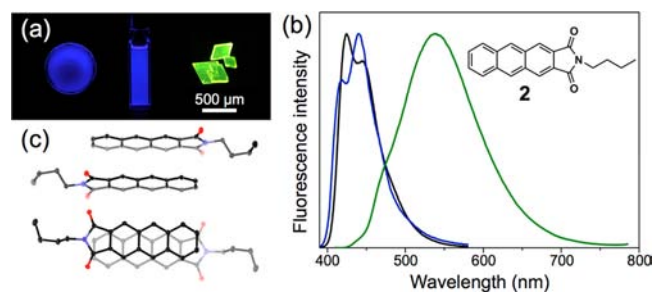


**Figure 5.** (a) Photographs and (b) spectra of the luminescence of **2** in PMMA matrix (left, blue line), in  $\text{CH}_2\text{Cl}_2$  (middle, black line), in crystals (right, green line).  $\lambda_{\text{ex}} = 300, 300,$  and  $400$  nm, respectively. (c)  $\pi$ -stacked dimer of **2** in crystals (50% probability for thermal ellipsoids).

other are reasonable for considering its rigid skeleton. In the crystalline state, this compound forms  $\pi$ -stacked dimers, showing an excimer emission ( $\tau = 88$  ns) with the  $\lambda_{\text{em}} = 538$  nm. However, the extent of the red shift ( $4140\text{ cm}^{-1}$ ) from that in the PMMA film is far smaller compared to **1** ( $5790\text{ cm}^{-1}$ ). Consequently, the emission color of the crystals was only greenish yellow. The significantly red-shifted excimer-like emission observed for **1** should be due to its characteristic two-fold  $\pi$ -stacked array structure, which may be more suitable for the formation of the contact excimer or the excited oligomer.<sup>16</sup>

In conclusion, we have designed and synthesized a  $\pi$ -conjugated system that consists of a flexible  $\pi$  joint and two

rigid  $\pi$  wings. This system shows two remarkable characteristics, namely (1) a dynamic conformational change in the excited state from a nonplanar V-shaped form to a planar form, leading to a dual fluorescence, and (2) a unique two-fold  $\pi$ -stacked array of the V-shaped molecules. These features result in generating each red, green, and blue emissive state based on a single luminophore, depending on its environment. The combination of a flexible scaffold and a rigid  $\pi$  skeleton is a potent versatile design of functional molecules, in which their dynamic motion would perturb not only optical properties, but also electrochemical, magnetic, and carrier-transporting properties.

## ■ ASSOCIATED CONTENT

### ■ Supporting Information

Experimental procedures; X-ray crystal structures (PDF, CIF) of **1** (CCDC-921157) and **2** (CCDC-921158); quantum chemical calculations; complete ref 13. This material is available free of charge via the Internet at <http://pubs.acs.org>.

## ■ AUTHOR INFORMATION

### Corresponding Author

s\_saito@chem.nagoya-u.ac.jp; sirle@chem.nagoya-u.ac.jp; yamaguchi@chem.nagoya-u.ac.jp

### Notes

The authors declare no competing financial interest.

## ■ ACKNOWLEDGMENTS

This work was supported by JST-PRESTO “Molecular technology and creation of new functions” to S.S, and JST-CREST to S.Y. The authors thank Dr. Hirofumi Yoshikawa and Prof. Kunio Awaga (Nagoya University) for help with the diffuse reflectance measurements. Crystallographic data collection was performed at the BL38B1 in the SPring-8 with approval of JASRI (proposal no. 2012B1324).

## ■ REFERENCES

- (1) (a) Beaujuge, P. M.; Fréchet, J. M. *J. Am. Chem. Soc.* **2011**, *133*, 20009. (b) Mishra, A.; Bäuerle, P. *Angew. Chem., Int. Ed.* **2012**, *51*, 2020. (c) Perepichka, I. F.; Perepichka, D. F. *Handbook of Thiophene-Based Materials*; vWiley-VCH: Weinheim, 2009.
- (2) (a) Anet, F. A. L. *J. Am. Chem. Soc.* **1962**, *84*, 671. (b) Nishinaga, T.; Ohmae, T.; Iyoda, M. *Symmetry* **2010**, *2*, 76.
- (3) (a) Seiders, T. J.; Baldrige, K. K.; Grube, G. H.; Siegel, J. S. *J. Am. Chem. Soc.* **2001**, *123*, 517. (b) Wu, Y.-T.; Siegel, J. S. *Chem. Rev.* **2006**, *106*, 4843.
- (4) (a) Sakurai, H.; Daiko, T.; Hirao, T. *Science* **2003**, *301*, 1878. (b) Amaya, T.; Sakane, H.; Muneishi, T.; Hirao, T. *Chem. Commun.* **2008**, 765.
- (5) Würthner, F. *Pure Appl. Chem.* **2006**, *78*, 2341.
- (6) (a) Stępień, M.; Sprutta, N.; Latso-Grażyński, L. *Angew. Chem., Int. Ed.* **2011**, *50*, 4288. (b) Saito, S.; Osuka, A. *Angew. Chem., Int. Ed.* **2011**, *50*, 4342.
- (7) (a) Marsella, M. J.; Reid, R. J.; Estassi, S.; Wang, L.-S. *J. Am. Chem. Soc.* **2002**, *124*, 12507. (b) Osswald, P.; Würthner, F. *Chem.—Eur. J.* **2007**, *13*, 7395. (c) Saito, S.; Shin, J. Y.; Lim, J. M.; Kim, K. S.; Kim, D.; Osuka, A. *Angew. Chem., Int. Ed.* **2008**, *47*, 9657. (d) Nishiuchi, T.; Kuwatani, Y.; Nishinaga, T.; Iyoda, M. *Chem.—Eur. J.* **2009**, *15*, 6838. (e) Mouri, K.; Saito, S.; Yamaguchi, S. *Angew. Chem., Int. Ed.* **2012**, *51*, 5971. (f) Nishiuchi, T.; Tanaka, K.; Kuwatani, Y.; Sung, J.; Nishinaga, T.; Kim, D.; Iyoda, M. *Chem.—Eur. J.* **2013**, *19*, 4110.
- (8) Lakowicz, J. R. *Principles of Fluorescence Spectroscopy*; Plenum Press: New York, 1999.

(9) (a) Hanson, J. C.; Nordman, C. E. *Acta Crystallogr., Sect. B* **1976**, *B32*, 1147. (b) Amaya, T.; Seki, S.; Moriuchi, T.; Nakamoto, K.; Nakata, T.; Sakane, H.; Saeki, A.; Tagawa, S.; Hirao, T. *J. Am. Chem. Soc.* **2009**, *131*, 408.

(10) (a) Rettig, W. *Angew. Chem., Int. Ed.* **1986**, *25*, 971. (b) Grabowski, Z. R.; Rotkiewicz, K.; Rettig, W. *Chem. Rev.* **2003**, *103*, 3899.

(11) Single-component systems that show each red, green, and blue (RGB) luminescence by changing the excitation energy: (a) Yang, Y.; Lowry, M.; Schowalter, C. M.; Fakayode, S. O.; Escobedo, J. O.; Xu, X.; Zhang, H.; Jensen, T. J.; Fronczek, F. R.; Warner, I. M.; Strongin, R. M. *J. Am. Chem. Soc.* **2006**, *128*, 14081. (b) Zhao, Y. S.; Fu, H.; Hu, F.; Peng, A. D.; Yao, J. *Adv. Mater.* **2007**, *19*, 3554. (c) He, G.; Guo, D.; He, C.; Zhang, X.; Zhao, X.; Duan, C. *Angew. Chem., Int. Ed.* **2009**, *48*, 6132.

(12) Multicolor emissions (rather than RGB) from a single luminophore: (a) Tong, H.; Hong, Y.; Dong, Y.; Ren, Y.; Häussler, M.; Lam, J. W. Y.; Wong, K. S.; Tang, B. Z. *J. Phys. Chem. B* **2007**, *111*, 2000. (b) Zhao, Y.; Gao, H.; Fan, Y.; Zhou, T.; Su, Z.; Liu, Y.; Wang, Y. *Adv. Mater.* **2009**, *21*, 3165. (c) Sagara, Y.; Kato, T. *Angew. Chem., Int. Ed.* **2011**, *50*, 9128. (d) Dong, Y.; Xu, B.; Zhang, J.; Tan, X.; Wang, L.; Chen, J.; Lv, H.; Wen, S.; Li, B.; Ye, L.; Zou, B.; Tian, W. *Angew. Chem., Int. Ed.* **2012**, *51*, 10782.

(13) DFT calculation of the inversion barrier was performed by the Gaussian program: Frisch, M. J.; et al. *Gaussian 09*, Revision C.01; Gaussian, Inc.: Wallingford, CT, 2010.

(14) (a) Lin, C.-H.; Lin, K.-H.; Pal, B.; Tsou, L.-D. *Chem. Commun.* **2009**, 45, 803. (b) Lin, Y.-C.; Lin, C.-H.; Chen, C.-Y.; Sun, S.-S.; Pal, B. *Org. Biomol. Chem.* **2011**, *9*, 4507.

(15) Excited-state calculations were performed by the TURBO-MOLE program: TURBOMOLE, ver. 6.3, 2012; a development of University of Karlsruhe and Forschungszentrum Karlsruhe GmbH, 1989–2007, TURBOMOLE GmbH, since 2007.

(16) Hinoue, T.; Shigenoi, Y.; Sugino, M.; Mizobe, Y.; Hisaki, I.; Miyata, M.; Tohnai, N. *Chem.—Eur. J.* **2012**, *18*, 4634.